Scientific Journal of University of Benghazi
SJUOB (2025) 38 (1) Applied Sciences: Alfarawi, et la , 112 – 128
www.sjuob.uob.edu.ly

A New CFD Approach to Predict Condensation Heat Transfer Coefficient of Steam Over a Horizontal Tube Using Apparent Heat Capacity Method

Suliman Alfarawi*,[1], Hossin Omar[1], Aynoor Elburki[2]

1.Department of Mechanical Engineering, University of Benghazi, Benghazi, Libya.
2 Department of Chemical Engineering, University of Benghazi, Benghazi, Libya.

Received: 28 / 02 / 2025 | Accepted: 11 / 04 / 2025 | Publishing: 29/06/2025

ABSTRACT

The present research paper aims to numerically solve fluid flow and heat transfer equation of a condensing steam over a single horizontal tube using computational fluid dynamics (CFD). The apparent heat capacity method is adopted in the current analysis which allows for the computation of a single-phase flow equation with an implicit capturing of the phase change interface between the vapor and liquid phases. A single energy equation is solved with effective material properties for the two phases based on the phase change temperature and the latent heat for the state change. The predicted heat transfer coefficient at different saturation temperatures [60, 80, 100 and 120 ºC] were initially compared to the results obtained from the well-known Nusselt analogy for laminar film condensation. It was found that the predicted heat transfer coefficient of 10429 W/m2. K at 60 ºC was 2% lower than that of Nusselt film analogy. While the predicted heat transfer coefficient of 11854 W/ m2. K at 120 ºC was 18% than that of Nusselt film analogy. Also, the results revealed that the heat transfer coefficient is merely dependent on the cross-flow velocity of the vapor and hence the vapor shear.

KEY WORDS: Apparent, Condensation, CFD, Heat capacity, Horizontal, Steam, Tube.

Corresponding Author: Suliman Alfarawi, suliman.alfarawi@uob.edu.ly

1.INTRODUCTION

Heat exchangers are devices that transfer heat between fluids at different temperatures. They are used in various applications, such as HVAC systems, power plants, and industrial processes. Heat exchangers can be classified in different ways. From a functional perspective, they include recuperative, regenerative, and direct mixing types. Based on transfer processes, they can be either direct contact or indirect contact. Another aspect is the flow arrangement which can be co-current, counter, or crossflow. Geometric construction options include tubular, plate, compact, and regenerative designs. Additionally, they can be categorized by fluid phases, such as condensers, evaporators, and crystallizers. The primary heat transfer mechanisms in heat exchangers are conduction, convection, and radiation. Conduction involves heat transfer through particle collisions, convection involves heat transfer through fluid movement, and radiation involves heat transfer through electromagnetic waves. Shell-and-tube heat exchangers (STHE) are most used in industry, and they are comprised of essential components such as shell, tubes, baffles, and nozzles as shown in Figure 1. These parts work together to enable efficient heat transfer between fluids. STHEs can be classified based on construction and service. Construction types include fixed tube sheet, U-tube, and floating head designs, while service types encompass single-phase, condensing, and vaporizing processes [1].

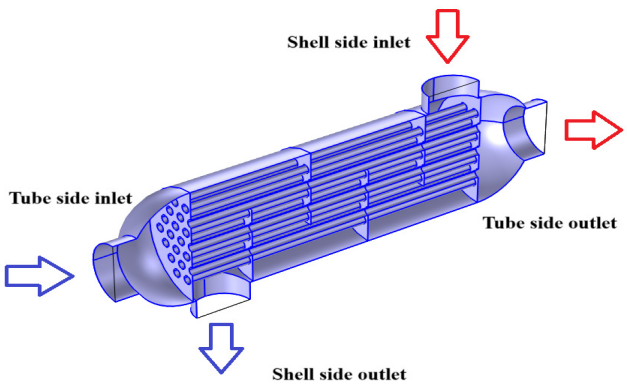

Figure. (1): Simple view of shell and tube counter flow heat exchanger.

Condensation inside a STHE occurs when a vapor, typically steam or refrigerant, comes into contact with a surface that is cooler than the vapor's dew point. This process is commonly used in various industrial applications for heat recovery, refrigeration, and power generation. The condensation process refers to the transformation of a substance from its gaseous phase into its liquid phase. This phase change occurs when a gas is cooled to its dew point or when the gas experiences an increase in pressure that forces it to condense. The heat released during this process is known as the latent heat of condensation. Condensation in a STHE may occur over the tube side or inside the tubes. However, in several designs, the vapor flows through the shell, and condensation occurs on the outer surfaces of the tubes as heat is transferred from the vapor to the cooler fluid flowing through the tubes. Condensation here results in liquid droplets forming on the tube surfaces, which then coalesce and drain due to gravity or flow-induced motion. Condenser surfaces may be wet with condensate, leading to film condensation, or non-wet, resulting in dropwise condensation. Film wise condensation as shown in Figure 2, forms a thin film of condensate on the surface of the tube.

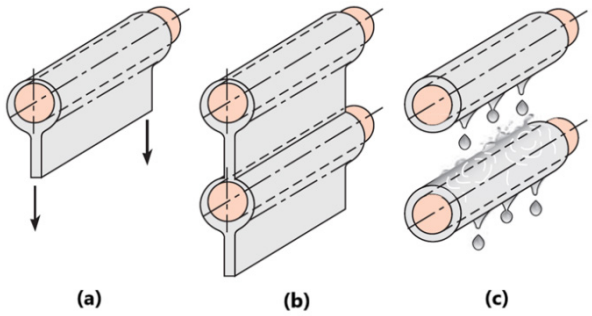

Figure. (2): Condensation over a tube, (*a*) a single horizontal tube, (*b*) a vertical tier of horizontal tubes with a continuous condensate sheet, and (*c*) with dripping condensate [1].

 ISSN: Online 2790-1637, Print 2790-1629
National Library of Libya, Legal number: 154/2018

This film can act as a thermal resistance, reducing the overall heat transfer rate. While, in dropwise condensation, drops of condensate are formed on the tube's surface which provides better heat transfer efficiency because it creates less resistance than film wise condensation inundation [1]. The vapor can be still or moving rapidly across the surface, and both the condensate and vapor may flow in laminar or turbulent patterns. Condenser design often relies on idealization and empirical methods. Even with a pure vapor, challenges like 3-D flow, turbulence, shear stress at the vapor-condensate interface, surface rippling, and inundation pose significant difficulties in making detailed modeling [2,3]. Theoretically, condensation is described by thermodynamic principles, which relates temperature, pressure, and phase changes of substances. Practically, researchers study condensation through controlled experiments in laboratories using equipment like condensers, dew point meters, and environmental chambers, simulating atmospheric or industrial conditions [4]. Steam condensation is a complex heat transfer process influenced by multiple factors, including the geometry of the tubes, flow patterns, steam properties, and operating conditions. Accurate modeling of these systems is essential for proper design and sizing, as simple models can lead to incorrect temperature differentials and underestimation of heat transfer area [5].

There is a growing need for detailed numerical investigations to provide more accurate predictions and efficient design of condensers. Fewer numerical studies exist in literature to predict fluid flow and heat transfer processes within an industrial shell and tube condenser. Marto [6] provided an extensive review on heat transfer and two-phase flow during shell-side condensation, focusing on historical developments, heat transfer enhancement, and computer modeling. Nusselt's laminar film condensation theory was a baseline model for condensation. His review covered various factors affecting heat transfer, including vapor shear, non-condensable gases, and enhancement techniques. Marto emphasized the need for further experimental data, particularly for large tube bundles, to refine correlations and improve predictive modeling.

Bonneau et al. [7] conducted a comprehensive review of pure vapor condensation outside horizontal smooth tubes, high-

lighting the diversity and accuracy of correlations for shell-side heat transfer coefficients. Their work reviewed Nusselt's foundational analysis on film condensation, emphasizing its limitations due to assumptions like stagnant vapor and laminar flow. They emphasized the influence of vapor shear stress and condensate inundation on heat transfer performance and more accurate and practical models are needed.

Ji et al. [8] investigated the condensation of refrigerants R134a and R22 in shell-and-tube condensers equipped with high-density low-fin tubes compared to 3D enhanced tubes. Their experiments revealed that the heat transfer coefficient for low-fin tubes was a 16.3–25.2% higher than that for traditional 3D enhanced tubes. They concluded that the overall refrigeration capacity remained comparable between different condenser designs, suggesting that low-fin tubes can provide substantial performance benefits while reducing material usage. However, potential maintenance challenges associated with high-density low-fin tubes may affect their practical application.

Mirzabeygi and Zhang [9] presented a numerical study on fluid flow and heat transfer on an industrial shell and tube condenser. The Eulerian–Eulerian approach was adopted in the analysis. Due to the 3D geometrical complexity in a full-size industrial condenser with an irregular shape, the tube bundle was modelled as porous media. With a considerable accuracy, the model was able to predict the condenser performance in terms of heat and mass transfer rates, pressure and temperature.

Doan et al. [10] conducted 3D numerical simulation and an experimental study on steam phase change in microchannel condensers. The apparent heat capacity method was adopted in the analysis. The numerical scheme reported lacks clarity in the formulations of the governing equations. However, they were able to get reasonable results in terms of phase change interface position compared to the experimental results. The authors demonstrated the correlation between steam mass flow rate and condensed water temperature on a limited range of mass flow rates from 0.01 g/s to 0.1 g/s, and specific geometric configuration.

El Ouali et al. [11] presented a dynamic model for latent cold thermal storage unit integrated with PCM spherical capsules.

The apparent heat capacity method was adopted. They showed that increasing the diameter of capsules from 47 mm to 77 mm increases the discharging period by about 30 %. However, heat transfer fluid flow rate and the capsule diameter must be properly investigated to minimize pumping power.

Due to the complexity and the computational resources needed for modelling such a problem using two-phase flow analysis with phase change heat transfer, the apparent capacity method is an alternative approach to explore. The apparent heat capacity method allows for the computation of a single-phase flow which is likely the vapor and provides an implicit capturing of the phase change interface between the vapor and liquid phases. A single energy equation is solved with effective material properties for the two phases based on the phase change temperature, the latent heat for the state change. The transition zone is carefully investigated to enable a smooth transition between the two phases (vapor and liquid).

Based on the previous studies reviewed in open literature, no detailed studies have been found related to the application of apparent heat capacity method in predicting condensation heat transfer coefficient for a single tube or a tube bundle of a heat exchanger. The research paper answers the question of what extent the apparent heat capacity method can be accurate in predicting the condensation of steam. The present work is aimed at numerically solving fluid flow and heat transfer of a condensing saturated vapor or a steam over a single horizontal tube using computational fluid dynamics (CFD) based on finite element analysis to predict the condensation heat transfer coefficient.

2.METHODS

Fluid flow and heat transfer with phase change analysis is conducted in this study using two-dimensional steady state non-isothermal flow formulation inside the environment of COMSOL Multiphysics version 6.2. The resulting governing equations are:

3.COMTINUITY EQUATION

$$\frac{\partial u}{\partial x} + \frac{\partial v}{\partial y} = 0 \quad -(1)$$

4.MOMENTUM EQUATION

$$u\frac{\partial u}{\partial x} + v\frac{\partial u}{\partial y} = -\frac{1}{\rho_{eff}}\frac{\partial p}{\partial x} + \frac{\mu_{eff}}{\rho_{eff}}\left(\frac{\partial^2 u}{\partial x^2} + \frac{\partial^2 u}{\partial y^2}\right) \quad --(2a)$$

 ISSN: Online 2790-1637, Print 2790-1629
National Library of Libya, Legal number: 154/2018

$$u\frac{\partial v}{\partial x}+v\frac{\partial v}{\partial y}=-\frac{1}{\rho_{eff}}\frac{\partial p}{\partial y}+\frac{\mu_{eff}}{\rho_{eff}}\left(\frac{\partial^2 v}{\partial x^2}+\frac{\partial^2 v}{\partial y^2}\right)+\rho_{eff}.g \quad -(2b)$$

where is the effective dynamic viscosity of the two phases and is calculated from.

$$\mu_{eff}=\mu_1\theta_1+\mu_2\theta_2 \quad --(3)$$

And is the effective density of the two phases calculated from

$$\rho_{eff}=\rho_1\theta_1+\rho_2\theta_2 \quad --(4)$$

The volume fractions of the two phases and are then calculated based on phase transition function as follows:

$$\theta_1=1-\alpha_{1\to 2} \quad --(5)$$

$$\theta_2=\alpha_{1\to 2} \quad --(6)$$

where θ_1 is the volume fraction of the material (vapor) before transition and θ_2 is the volume fraction of the material (liquid) after transition. The phase transition from phase 1 to phase 2 is described by the phase transition function, . The phase transition function shown in Figure 3 is a smoothed step function with a continuous second derivative (Heaviside function) changes from 0 before phase change temperature T_{pc} to 1 after phase change temperature T_{pc}.

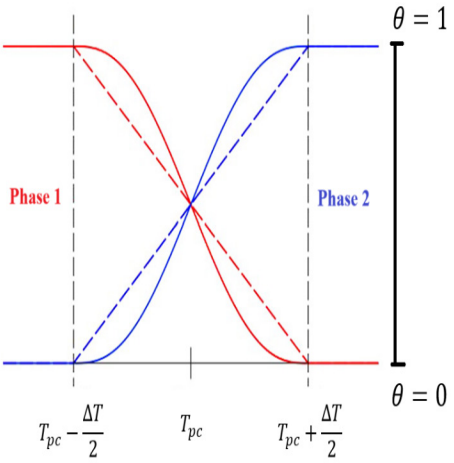

Figure. (3): Phase volume fractions using Heaviside function [12].

The effective thermal conductivity of the two phases is calculated from

$$k_{eff}=k_1\theta_1+k_2\theta_2 \quad --(7)$$

5.ENERGY EQUATION

$$u\frac{\partial T}{\partial x}+v\frac{\partial T}{\partial y}=\frac{k_{eff}}{\rho_{eff}C_p}.\left(\frac{\partial^2 T}{\partial x^2}+\frac{\partial^2 T}{\partial y^2}\right)-(8)$$

where and , are effective thermal conductivity and apparent heat capacity, respectively. According to the formulation of apparent heat capacity method [12], the apparent heat ca-

pacity is obtained by summing up the equivalent heat capacity of the two phases and latent heat distribution as follows

$$C_p = \frac{1}{\rho_{eff}}\left(\rho_1\theta_1 C_{p,1} + \rho_2\theta_2 C_{p,2}\right) + L\frac{d\alpha_m}{dT} \text{--(9)}$$

where L is the latent heat of vaporization and is the mass fraction and is calculated from

$$\alpha_m = 0.5\frac{\rho_2\theta_2 - \rho_1\theta_1}{\rho_{eff}} \text{--(10)}$$

5.1.Model set up

The CFD model was set up in COMSOL Multiphysics to calculate the heat transfer coefficient of a condensing saturated steam on the outer surface of horizontal 6 mm diameter single tube at different saturation temperatures ranging from 60 to 120 ºC.

The 2D computational domain is 18 mm in width and 24 mm in hight with a centred hollow circle of 6 mm diameter which represents water cooling tube. The tube of cooling water is treated as an isothermal tube and its wall is maintained at 25 ºC. The 2D computational domain and applied boundary conditions BCs are depicted in Figure 4. To ensure a laminar vapor flow, a fully developed flow boundary condition with an inlet velocity of 10 mm/s was selected and fixed for all simulation cases. The reference pressure was fixed to 1 [bar] for all cases to calculate vapor density at different saturation temperatures while the outlet pressure is set to zero pressure (relative pressure).

The heat transfer with phase change is enabled with inlet temperature of the vapor and constant wall temperature of the tube at 25 ºC. Outflow boundary conditions are applied at the outlet of the domain. The 2D computational domain was meshed with free triangular elements and two boundary layers sequence around the surface of the horizontal tube to resolve velocity and temperature gradients around the tube.

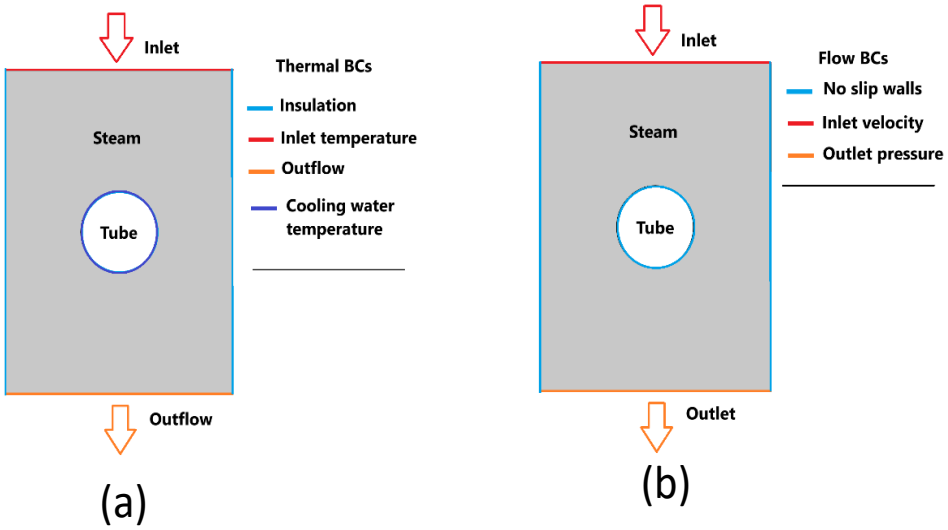

Figure. (4): 2D computational domain with applied boundary conditions, (a) flow BCs, (b) thermal BCs.

All simulations were performed on Intel® core™ CPU i7-10610U runs at a speed of 2.3 GHz with 16 GB RAM memory. The sensitivity analysis of the mesh size on the predicted heat transfer coefficient was illustrated in Table (1).

It can be seen that the result of heat transfer coefficient is relatively sensitive to further refining the mesh size. However, the result of heat transfer coefficient is strongly affected by the transition interval, ΔT. As the transition interval becomes smaller, a finer mesh is needed for smooth transition during phase change.

Table .(1): Mesh sensitivity analysis

Grid No	No of elements	HTC (W/m^2. K)	Deviation %
1	7054	12615	-
2	18774	10876	13%
3	29262	10429	4%

 ISSN: Online 2790-1637, Print 2790-1629
National Library of Libya, Legal number: 154/2018

Table (2) shows the variation of heat transfer coefficient (HTC) with the temperature interval ΔT at a fixed grid size (No 3). The solver started with a wide temperature interval of 50 K so that the final solution for the current temperature interval is the initial guess to the next temperature interval and ramped down to a smaller value of 10 K. This ensures a smooth converged transition of the phase from vapor to liquid at the predefined phase change temperature. As can be seen the value of HTC stabilizes at a lower temperature interval of 10 K with a deviation less than 1%. This confirms the temperature interval of 10 K satisfies energy and mass conservation in phase change model.

Table .(2): Variation of heat transfer coefficient (HTC) with the temperature interval ΔT at a fixed grid size.

ΔT	HTC (W/m². K)	Deviation %
50 K	12661	-
40 K	11807	6.7%
30 K	10836	8.2%
20 K	10507	3%
10 K	10429	<1%

6.RESULTS AND DISCUSSION

6.1.Model validation

Several researchers have compared condensation heat transfer coefficient obtained from Nusselt analysis (Rewritten below) with experimental data for a single tube, using a variety of test fluids, and agreement within 30% has often been reported [6].

$$\bar{h}_D = 0.729\left[\frac{\rho_l g(\rho_l-\rho_v)k_l^{\,3}h_{fg}}{\mu_l(T_{sat}-T_s)D}\right] \text{--(11)}$$

The comparison with Nusselt equation illustrated in Table 4 showed a fairly good agreement within [2-18] % deviation which gives a confidence in the adopted numerical procedure. However, the deviation may be attributed to the fact that the current CFD model accounts for vapor velocity (vapor shear) and temperature-dependent properties when compared to the idealized Nusselt analysis.

Table .(3): Comparison of heat transfer coefficient (HTC) with Nusselt equation [6].

Saturation temperature (C°)	Heat transfer coefficient (HTC) (W/m^2. K)		Deviation
	CFD	Nusselt eq'n [11]	
60	10429	10679	2%
80	11050	10059	9%
100	11518	9775	15%
120	11854	9677	18%

6.2.General results

The results for velocity, pressure, temperature and phase profiles at a saturation temperature of 60 ºC are demonstrated in Figure 5. The velocity and pressure profiles (Figure 5a and 5b) resemble the steady fluid flow over a cylinder where the highest pressure is the stagnation pressure which is very small corresponding to the vapor inlet velocity of 10 mm/s. The inlet vapor temperature in this case is 65 ºC (Figure 5c) and only temperature gradient is exhibited at the wall of cooling tube. The sensible cooling starts until the phase change temperature of 60 ºC is reached near the tube wall then phase change occurs. As depicted in Figure 5d, the phase interface captures the formation of film condensation.

 ISSN: Online 2790-1637, Print 2790-1629
National Library of Libya, Legal number: 154/2018

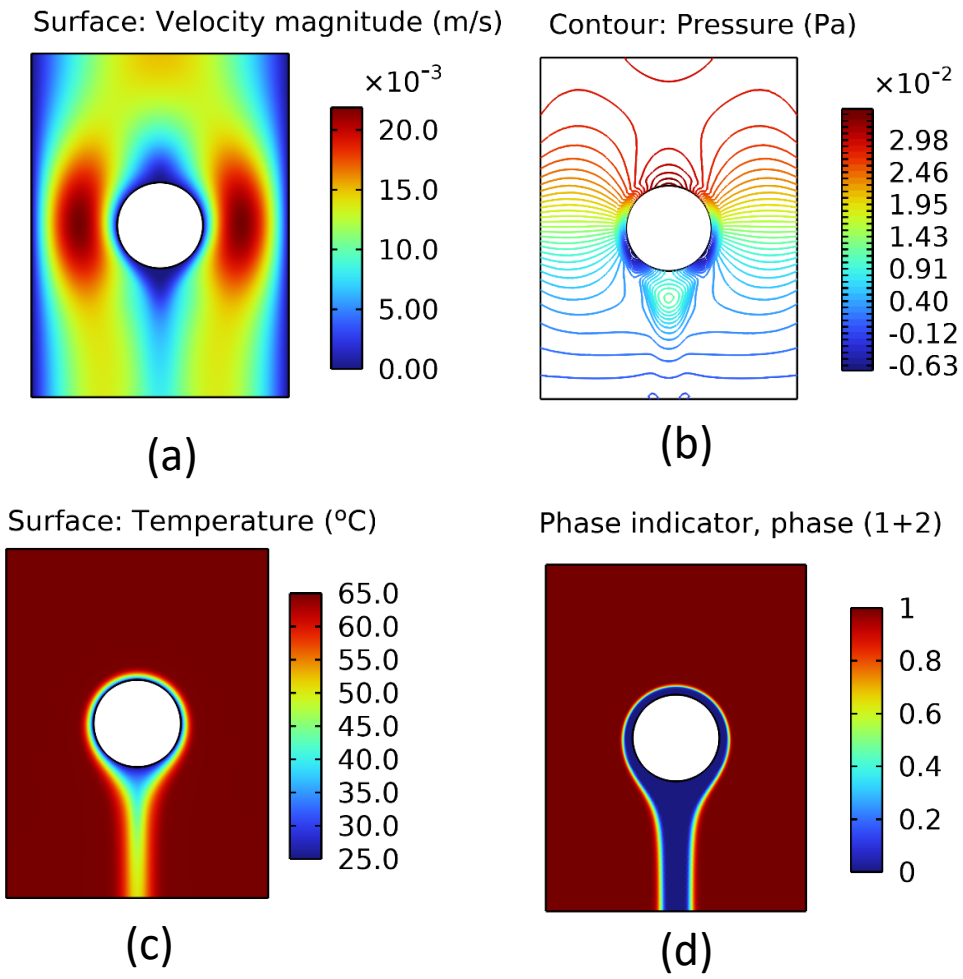

Figure.(5): CFD results of a condensing steam over a horizontal tube, (a) velocity, (b) pressure, (c) temperature and (d) phase indicator.

6.3.Effect of vapor velocity

In this section, the effect of vapor velocity on the condensation heat transfer coefficient was investigated. Previous studies, as reviewed by Browne and Bansal [13] reported that the forced-convection condensation is proportional to the magnitude of the cross-flow velocity. Therefore, the simulations were carried out with a varied vapor inlet velocity from 5 mm/s to 20 mm/s for the case of saturation temperature of 60 ºC. The corresponding cross-flow velocity profiles are plotted in Figure 6(a). As can be seen, the cross-flow velocity profile is a result of the no-slip boundary conditions at positions x = 3 mm and x = 9 mm of the tube wall and the vertical wall, respectively and the maximum cross-flow velocity at a position of x = 5.6844 mm. The cross-flow velocity is almost a two-folds of the vapor inlet velocity as depicted in Figure 6(b). The existence of vapor shear due to the established velocity gradient near the tube wall strongly affects the condensing heat transfer coefficient. Figure 6(c) shows an increasing trend of HTC to the power of (0.4526) of the maximum cross-flow velocity.

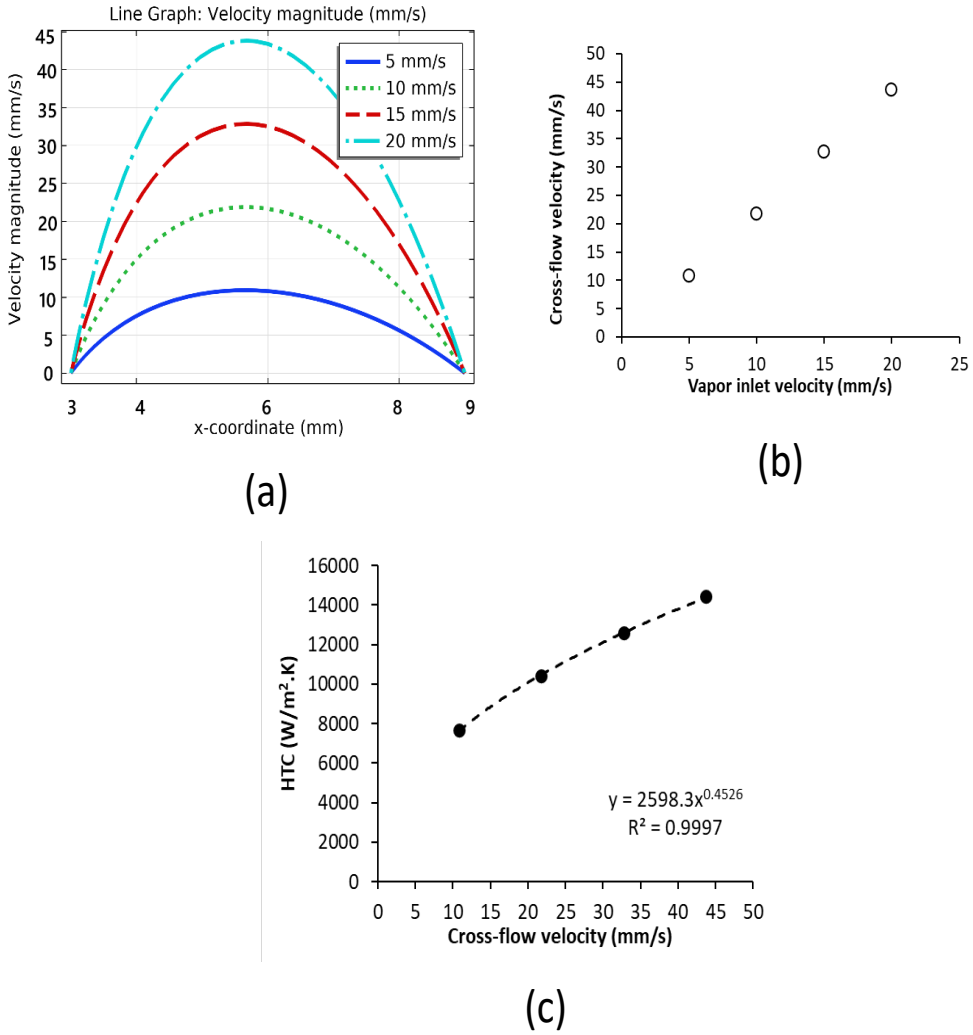

Figure.(6): Effect of vapor velocity on forced-convection condensation, (a) cross-flow velocity profile, (b) variation of cross-flow velocity with vapor inlet velocity (c) HTC.

In order to understand how the HTC increases with respect to the vapor shear, the phase indicators at different vapor inlet velocities were visualized as depicted in Figure 7. As expected, the increase in vapor shear causes a thinning in the film thickness of the condensate when the inlet velocity increases from 5 mm/s to 20 mm/s. Therefore, the conductive thermal resistance of the condensate decreases when the inlet velocity increases resulting in higher values of HTC. This observation is in line with theory and previous studies [13, 14].

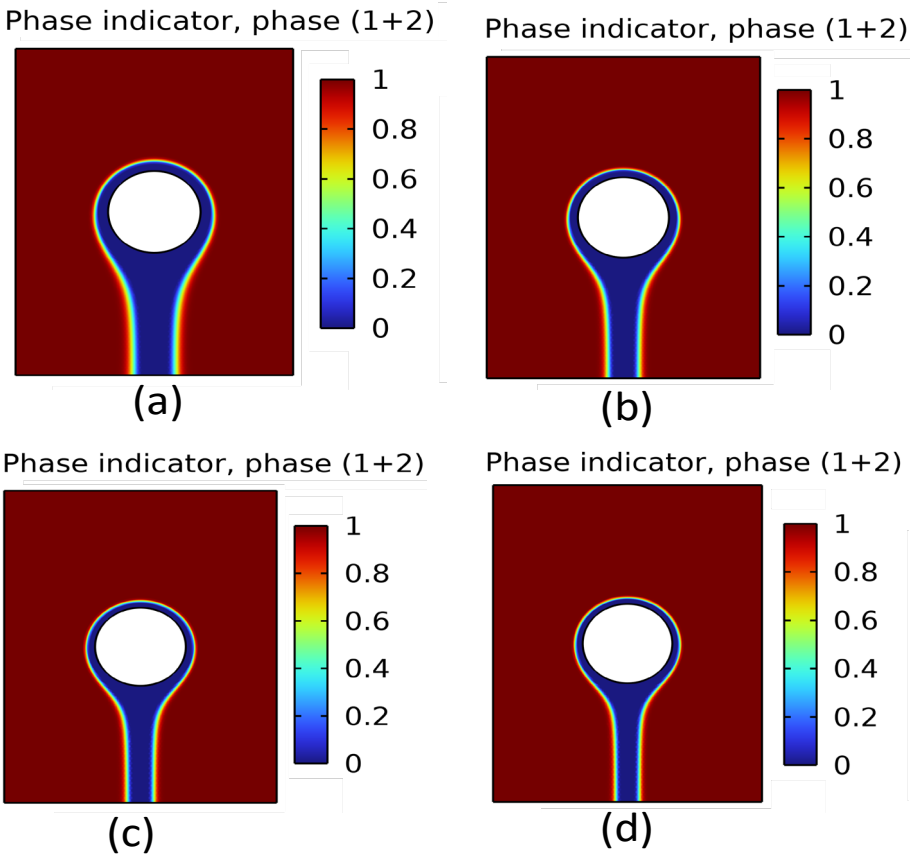

Figure.(7): Effect of vapor velocity on condensing steam over a horizontal tube, (a) v = 5 mm/s, (b) v = 10 mm/s, (c) v = 15 mm/s and (d) v = 20 mm/s.

7.CONCLUSIONS

A new CFD approach based on apparent heat capacity method was proposed to predict the condensation heat transfer coefficient of steam over a single horizontal tube. The model was validated against Nusselt film analogy at different saturation temperatures with reasonable accuracy. The effect of vapor velocity on the condensation heat transfer coefficient was presented. The current model is robust, computationally inexpensive and can be further extended for future work to account for the inundation phenomenon in real tube bundle of a condenser.

8.REFERENCES

[1] Bergman TL, Lavine AS, Incropera FP, DeWitt DP. Introduction to heat transfer. John Wiley & Sons; 2011.

[2] Kakaç S, Bergles AE, Fernandes EO, editors. Two-phase flow heat exchangers: Thermal-hydraulic fundamentals and design. Springer Science & Business Media; 2012.

[3] Nitsche M, Gbadamosi RO. Heat exchanger design guide: a practical guide for planning, selecting and designing of shell and tube exchangers. Butterworth-Heinemann; 2015.

[4] Pekař L. Introduction to heat exchangers. In Advanced Analytic and Control Techniques for Thermal Systems with Heat Exchangers 2020. (pp. 3-20). Academic Press.

[5] Luyben WL. Reality versus simulation-implementation of heat exchangers with phase changes. Computers & Chemical Engineering. 2023; 175:108284. https://doi.org/10.1016/j.compchemeng.2023.108284

[6] Marto PJ. Heat transfer and two-phase flow during shell-side condensation. Heat Transfer Engineering. 1984;5(1-2):31-61. https://doi.org/10.1080/01457638408962767

[7] Bonneau C, Josset C, Melot V, Auvity B. Comprehensive review of pure vapour condensation outside of horizontal smooth tubes. Nuclear Engineering and Design. 2019; 349:92-108. https://www.sciencedirect.com/science/article/pii/S0029549319300718

[8] Ji WT, Zhao CY, Lofton J, Li ZY, Zhang DC, He YL, Tao WQ. Condensation of R134a and R22 in shell and tube condensers mounted with high-density low-fin tubes. Journal of Heat Transfer. 2018;140(9):091503. https://doi.org/10.1115/1.4040083

[9] Mirzabeygi P, Zhang C. Three-dimensional numerical model for the two-phase

flow and heat transfer in condensers. International Journal of Heat and Mass Transfer. 2015; 81:618-637. https://doi.org/10.1016/j.ijheatmasstransfer.2014.10.015

[10] Doan M, Le T, Dang T, Teng JT. A Numerical Simulation on Phase Change of Steam in a Microchannel Condenser. International Journal of Power and Energy Research. 2017;1(2). https://dx.doi.org/10.22606/ijper.2017.12005

[11] El Ouali A, Khattari Y, Lamrani B, El Rhafiki T, Zeraouli Y, Kousksou T. Apparent heat capacity method to describe the thermal performances of a latent thermal storage system during discharge period. Journal of Energy Storage. 2022; 52:104960. https://doi.org/10.1016/j.est.2022.104960

[12] COMSOL Multiphysics, Heat transfer Module User's Guide, Chapter 4 -Theory for the heat transfer module: 206-211. COMSOL 6.2.

[13] Browne MW, Bansal PK. An overview of condensation heat transfer on horizontal tube bundles. Applied Thermal Engineering. 1999;19(6):565-694. https://doi.org/10.1016/S1359-4311(98)00055-6

[14] Kutateladze SS, Gogonin II. Heat transfer in condensation of flowing vapour on a single horizontal cylinder. International journal of heat and mass transfer. 1985; 28(5):1019-1030. https://doi.org/10.1016/0017-9310(85)90284-4